

# Distinct brain network features predict internalizing and externalizing traits in children, adolescents and adults

Received: 24 May 2023

Accepted: 15 January 2025

Published online: 19 February 2025

 Check for updates

Yueyue Lydia Qu <sup>1,2</sup>✉, Jianzhong Chen<sup>3,4,5,6</sup>, Angela Tam<sup>3,4,5,6</sup>, Leon Qi Rong Ooi<sup>3,4,5,6,7</sup>, Elvisha Dhamala <sup>8</sup>, Carrisa V. Cocuzza<sup>1,2</sup>, Shaoshi Zhang <sup>3,4,5,6</sup>, Tianchu Zeng<sup>3,4,5,6</sup>, Connor Lawhead<sup>1</sup>, B. T. Thomas Yeo <sup>3,4,5,6,7,9</sup> & Avram J. Holmes <sup>10</sup>✉

The distinction between externalizing and internalizing traits has been a classic area of study in psychiatry. However, whether shared or unique brain network features predict internalizing and externalizing behaviors remains poorly understood. Using a sample of 5,260 children from the Adolescent Brain Cognitive Development study, 229 adolescents from the Healthy Brain Network and 423 adults from the Human Connectome Project, we show that predictive network features are, at least in part, distinct across internalizing and externalizing behaviors. Across all three samples, behaviors within internalizing and externalizing categories exhibited more similar predictive feature weights than behaviors between categories. These data suggest shared and unique brain network features account for individual variation within broad internalizing and externalizing categories across developmental stages.

The distinction between ‘internalizing’ and ‘externalizing’ behaviors has been a classic area of study in child and adolescent psychiatry<sup>1</sup>. Internalizing behaviors are directed toward the individual and manifest in their extreme form as sadness, withdrawal, somatic complaints and anxiety, while externalizing behaviors are directed toward the environment or others and involve disruptive and aggressive behaviors<sup>2</sup>. These behaviors have been linked to increased risk for suicide attempts in childhood and adolescence<sup>3,4</sup> as well as worse work performance and lower cognitive abilities in adulthood<sup>5,6</sup>. However, the neural underpinnings associated with internalizing and externalizing behaviors across developmental stages remain poorly understood.

Throughout development, functional connectivity (FC) patterns within and between large-scale brain networks can predict individual differences in cognition<sup>7</sup>, impulsivity<sup>8</sup> and psychiatric symptoms<sup>9,10</sup>.

While individual-level variability in the organization of large-scale brain networks can predict individual differences within broad categories of cognition, personality and mental health in both children and adults<sup>11,12</sup>, macroscale patterns of brain functioning are dynamic across the lifespan<sup>13–15</sup>. Therefore, it is unclear whether the specific brain–behavior relationships observed in childhood mirror those in other developmental stages. Furthermore, although shared network features account for individual variation within broad classes of behavior<sup>11</sup>, individual-specific patterns of functional network connections may predict even finer-grained categories, such as internalizing and externalizing. In this Article, we examine the extent to which brain-based predictors of internalizing and externalizing behaviors are similar across a large sample of children and independent samples of adolescents and young adults.

<sup>1</sup>Department of Psychology, Yale University, New Haven, CT, USA. <sup>2</sup>Wu Tsai Institute, Yale University, New Haven, CT, USA. <sup>3</sup>Center for Sleep and Cognition, National University of Singapore, Singapore, Singapore. <sup>4</sup>Center for Translational MR Research, National University of Singapore, Singapore, Singapore. <sup>5</sup>Department of Electrical and Computer Engineering, National University of Singapore, Singapore, Singapore. <sup>6</sup>N.1 Institute for Health and Institute for Digital Medicine (WisDM), National University of Singapore, Singapore, Singapore. <sup>7</sup>Integrative Sciences and Engineering Programme (ISEP), National University of Singapore, Singapore, Singapore. <sup>8</sup>Institute of Behavioral Sciences, Feinstein Institutes for Medical Research, Manhasset, NY, USA. <sup>9</sup>Martinos Center for Biomedical Imaging, Massachusetts General Hospital, Charlestown, MA, USA. <sup>10</sup>Department of Psychiatry, Brain Health Institute, Rutgers University, Piscataway, NJ, USA. ✉e-mail: [lydia.qu@yale.edu](mailto:lydia.qu@yale.edu); [avram.holmes@rutgers.edu](mailto:avram.holmes@rutgers.edu)

In the present study, we predicted internalizing and externalizing measures of psychopathology in a sample of children from the Adolescent Brain Cognitive Development (ABCD) study<sup>16</sup> from their resting-state functional connectivity (RSFC) matrices using kernel ridge regression (KRR) models (Supplementary Methods 1). We further explored RSFC predictors of internalizing and externalizing in an independent cohort of adolescents from the Healthy Brain Network (HBN)<sup>17</sup> and an independent cohort of young adults from the Human Connectome Project (HCP)<sup>18</sup>. Across all three samples, the exact test of differences<sup>19</sup> revealed that network features more similarly predicted pairs of behavioral measures within either the internalizing or the externalizing category than those across categories, supporting internalizing and externalizing behaviors as distinct factors of psychopathology across datasets characterized by distinct developmental stages. Specifically, predictive network features that are significantly different between internalizing and externalizing behavior in ABCD children and HBN adolescents involve primarily functional connections to the subcortical regions and the visual network from other large-scale functional networks, with HBN adolescents characterized by more distributed patterns. However, predictive network features that are significantly different between internalizing and externalizing behavior in HCP adults involve primarily FC within large-scale canonical networks. These results further suggested that functional network features differentially predicting internalizing and externalizing behavior may change across the lifespan.

## Results

### Imaging and behavioral data

To examine brain-based predictive network features of internalizing and externalizing behavior in children, we considered resting-state functional magnetic resonance imaging (rsfMRI) data from  $N = 11,875$  typically developing children (ABCD 2.0.1 release<sup>16</sup>). The final analytical sample consisted of  $n = 5,260$  unrelated children with complete data who passed fMRI quality control (Methods and Supplementary Tables 1 and 2). Our analyses considered six measures of internalizing and externalizing behavior (Supplementary Table 3)<sup>20</sup>, assigning three to the child internalizing category and three to the child externalizing category (Supplementary Table 4).

To assess the generalizability of our ABCD results to other developmental stages such as adolescence and adulthood, we additionally examined brain-based predictive network features of internalizing and externalizing behavior in an independent sample of adolescents and adults. Specifically, we analyzed rsfMRI data and measures of internalizing and externalizing behavior from 229 HBN adolescents (HBN releases 1–7 (ref. 17)) and 423 HCP young adults (HCP S1200 data release<sup>18</sup>). In the HBN sample (Supplementary Table 5), we analyzed the same measures as in the ABCD sample (Supplementary Table 6) and assigned them similarly to adolescent internalizing and externalizing categories (Supplementary Table 7).

In the HCP sample (Supplementary Table 8), we considered six measures assessing the same set of internalizing and externalizing behaviors in adults (Supplementary Table 9)<sup>21</sup>, assigning them similarly to adult internalizing and externalizing categories (Supplementary Table 10). Both samples were not significantly different from the ABCD sample in their levels of total internalizing and externalizing problems (Supplementary Tables 11 and 12).

### Evidence for brain–behavior KRR prediction in ABCD children

Across all samples, we defined 400 cortical<sup>22</sup> and 19 subcortical<sup>23</sup> regions of interest (ROIs)<sup>23,24</sup> and estimated a 419 by 419 RSFC matrix (Fig. 1a,b). Following previous work<sup>11</sup>, we used KRR models to predict each behavioral measure from subject-specific RSFC matrices in each sample. To evaluate predictive accuracy, we performed nested cross-validation procedures (Methods). Pearson's correlations between

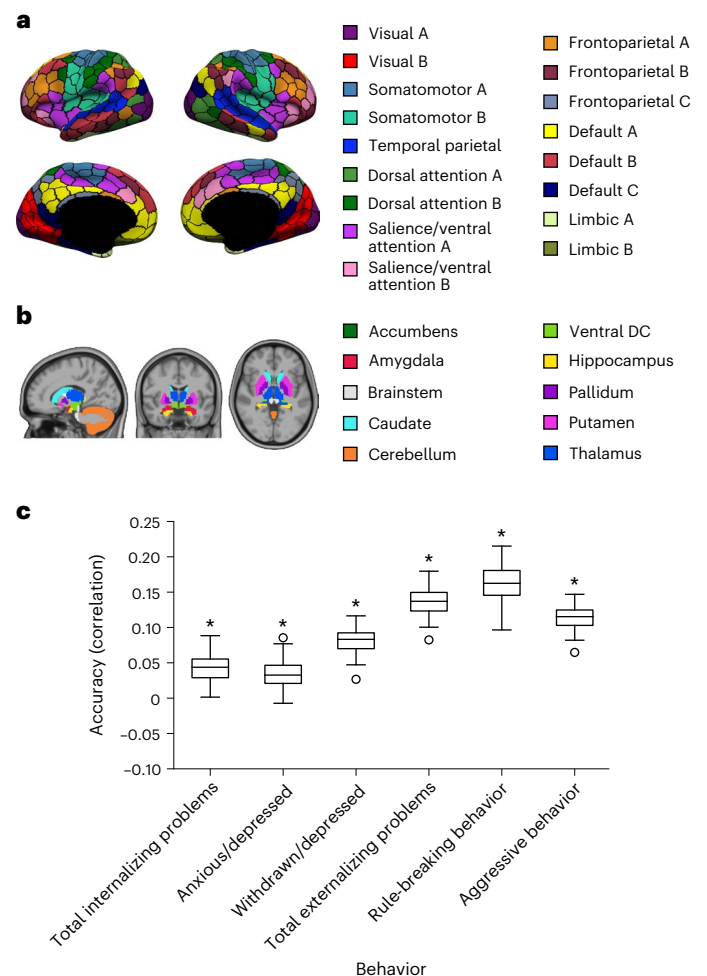


**Fig. 1 | Whole-brain FC predicts internalizing and externalizing behaviors in ABCD children.** **a**, Four hundred cortical ROIs<sup>22</sup> and their assignment to one of 17 large-scale networks<sup>30</sup>. **b**, Nineteen subcortical ROIs<sup>23</sup>. **c**, KRR prediction performance in ABCD children. For each box plot, the top and bottom edges represent upper and lower quartiles of correlation coefficient ( $r$ ) distributions, and the horizontal line marks the median. Outliers are plotted as circles. Asterisks (\*) denote above-chance significance on the basis of permutation testing after FDR correction ( $q < 0.05$ ). Panels reproduced from: **a**, ref. 84 under a Creative Commons license [CC BY 4.0](https://creativecommons.org/licenses/by/4.0/); **b**, ref. 85 under a Creative Commons license [CC BY 4.0](https://creativecommons.org/licenses/by/4.0/).

predicted and actual behavioral scores were used as accuracy metrics. Statistical significance of prediction accuracy was assessed by permutation testing. All behavioral measures in the ABCD sample were predicted better than chance after false discovery rate (FDR) correction (Fig. 1c;  $q < 0.05$ ). Notably, prediction accuracy is generally low (Pearson's  $r = 0.03$ – $0.16$ ). This is consistent with recent work by Marek and colleagues that demonstrated that the effect size of the association between RSFC and measures of psychopathology is subtle ( $r = -0.05$ – $0.05$ ) across multiple large-scale datasets<sup>24</sup>.

By contrast, none of the behavioral measures from the HBN or the HCP sample achieved better-than-chance accuracy (Supplementary Figs. 1 and 2). These two samples have relatively smaller sample sizes, thus not affording sufficient power for detecting such brain–behavior relationships with low effect sizes.

### Distinct FC predictors between categories across all samples

Here we sought to determine whether internalizing and externalizing behaviors exhibited distinct patterns of predictive feature weights across datasets. At each cross-validation fold, we quantified the ‘feature importance’ of each interregional RSFC edge, predicting each behavior

using Haufe's transformation (Methods)<sup>25</sup>, yielding a 419 × 419 predictive feature weight matrix for each behavior in each sample.

Next, consistent with previous work<sup>26,27</sup>, we analyzed whether predictive feature weights computed from KRR model outputs were more similar among behaviors within versus between internalizing and externalizing categories using the exact test of differences<sup>19</sup>. We conducted exact tests of differences between pairs of predictive weight vectors associated with each RSFC edge, predicting different pairs of behavioral measures across all cross-validation folds. In each sample, we assessed whether predictive feature weights associated with behavioral pairs within the same categories were more similar (that is, significantly different across a lower proportion of RSFC edges out of all 87,571 RSFC edges) than predictive feature weights associated with behavioral pairs across different categories (Methods).

In ABCD children, the proportions of RSFC edges exhibiting significantly different predictive feature weights were higher between each internalizing subscale and Total Child Externalizing Problems Scale (48.4% and 16.7% of edges) than between the two internalizing subscales (0.42%; Fig. 2a). Further, the proportions of edges exhibiting significantly different predictive feature weights were higher between each externalizing subscale and Total Child Internalizing Problems Scale (37.3% and 29.1%) than between the two externalizing subscales (20.0%; Fig. 2a). Since internalizing and externalizing measures were reported by different family members across ABCD children, we repeated these analyses within the subset of children whose behavioral measures were reported by their mothers and observed a consistent pattern of results (Supplementary Fig. 3).

In both HBN adolescents and HCP adults, the patterns we observed were broadly consistent with the ABCD results. The proportions of RSFC edges exhibiting significantly different predictive feature weights were higher between each internalizing subscale and Total Externalizing Problems Scale (51.4% and 47.3% in HBN (Fig. 2b); 41.8% and 39.9% in HCP (Fig. 2c)) than between the two internalizing subscales (0.69% in HBN (Fig. 2b); 0.54% in HCP (Fig. 2c)). Moreover, the proportions of edges exhibiting significantly different predictive feature weights were higher between each externalizing subscale and Total Internalizing Problems Scale (41.8% and 47.8% in HBN (Fig. 2b); 48.4% and 41.0% in HCP (Fig. 2c)) than between the two externalizing subscales (33.7% in HBN (Fig. 2b); 23.6% in HCP (Fig. 2c)). These results suggest that brain-based predictive features within internalizing and externalizing categories are more similar than predictive features between these categories across ABCD children, HBN adolescents and HCP adults. Overall, brain network features predicting behaviors within the same category are more similar to each other than to those predicting behaviors from the other category across datasets characterized by distinct developmental stages.

Previous work showed that predictive features are generally similar across mental health measures<sup>11</sup>. Our findings showed that beyond this broad pattern of similarity within the general domain of mental health, predictive feature weights were more similar within than between internalizing and externalizing categories across multiple datasets with different age groups. These findings are consistent with theoretical models that consider internalizing and externalizing behaviors as distinct constructs of psychopathology under a general psychopathology *p* factor<sup>28,29</sup>.

### Network blocks with distinct FC predictors within each sample

Having established that distinct RSFC features drive the prediction of total internalizing and externalizing problems across distinct developmental stages, we next examined which networks contained the largest proportions of RSFC edges whose associated predictive feature weights were significantly different between total internalizing and externalizing problems in each developmental stage. We listed out the top five network blocks in terms of the proportions of FC edges that significantly predicted Total Internalizing Problems Scale and

Total Externalizing Problems Scale in each sample (Supplementary Tables 13–15).

Among ABCD children, network blocks containing the highest proportions of RSFC edges with significantly more positive or less negative feature weights when predicting total internalizing problems than predicting total externalizing problems involved primarily functional connections from the other networks to the subcortical regions. High proportions of RSFC edges within attention and frontoparietal networks also predicted total internalizing problems more positively or less negatively than total externalizing problems. However, network blocks containing high proportions (>50%) of RSFC edges with significantly more positive or less negative feature weights when predicting total externalizing problems than predicting total internalizing problems involved predominantly between-network connectivity to the visual network (Fig. 3 and Supplementary Table 13).

In HBN adolescents, network blocks containing the highest proportions of RSFC edges that predicted total internalizing problems more positively or less negatively similarly involved between-network functional connections to the subcortical regions, while high proportions of RSFC edges that predicted total externalizing problems more positively or less negatively can be similarly found in network blocks involving the visual network. On top of these overlapping patterns with ABCD results, high proportions of between-network functional connections between the attention networks and other networks additionally emerged as different predictors of total internalizing and externalizing problems (Fig. 3 and Supplementary Table 14).

In HCP adults, the majority of predictive edges are found within rather than between functional networks, although high proportions of RSFC edges differently predicting total internalizing and externalizing problems can still be found in a few between-network functional connections involving subcortical regions and the visual network (Fig. 3 and Supplementary Table 15).

Across all three samples, the highest proportions of RSFC predictors that predicted total internalizing problems more positively or less negatively than total externalizing problems can be found between the temporal-parietal network and the subcortical regions. These results suggest that more positive or less negative FC between the temporal-parietal network and the subcortical regions may be a specific predictor of internalizing behavior across distinct developmental stages. Distinct RSFC predictors of internalizing and externalizing behavior in adulthood may be more evident within large-scale functional networks, while they may be more represented in between-network functional connections involving visual network and subcortical regions in childhood and adolescence.

### Directionality of network FC prediction within each sample

While the previous section identified network blocks that most differently predicted total internalizing and externalizing problems scores in each sample, it is not clear whether stronger predictions of one score were driven by highly positive predictive feature weights within these network blocks predicting the score or highly negative predictive feature weights associated with the other score, or both. Hence, in this section we determined whether any of the network blocks identified in the previous section also drive the positive or negative prediction of total internalizing and externalizing problems in the corresponding sample where they emerged as the strongest differential predictors.

To determine the specific RSFC features that consistently predicted total internalizing and externalizing problems, we performed permutation tests and visualized statistically significant feature weights associated with predicting total internalizing problems and total externalizing problems in each sample. To limit the number of multiple comparisons and allow inferences about well-replicated, functionally relevant large-scale brain systems, predictive feature weights for each behavior were averaged within and between 18 functional modules (following the 17-network partition in ref. 30 plus subcortical structures<sup>23</sup>) at each

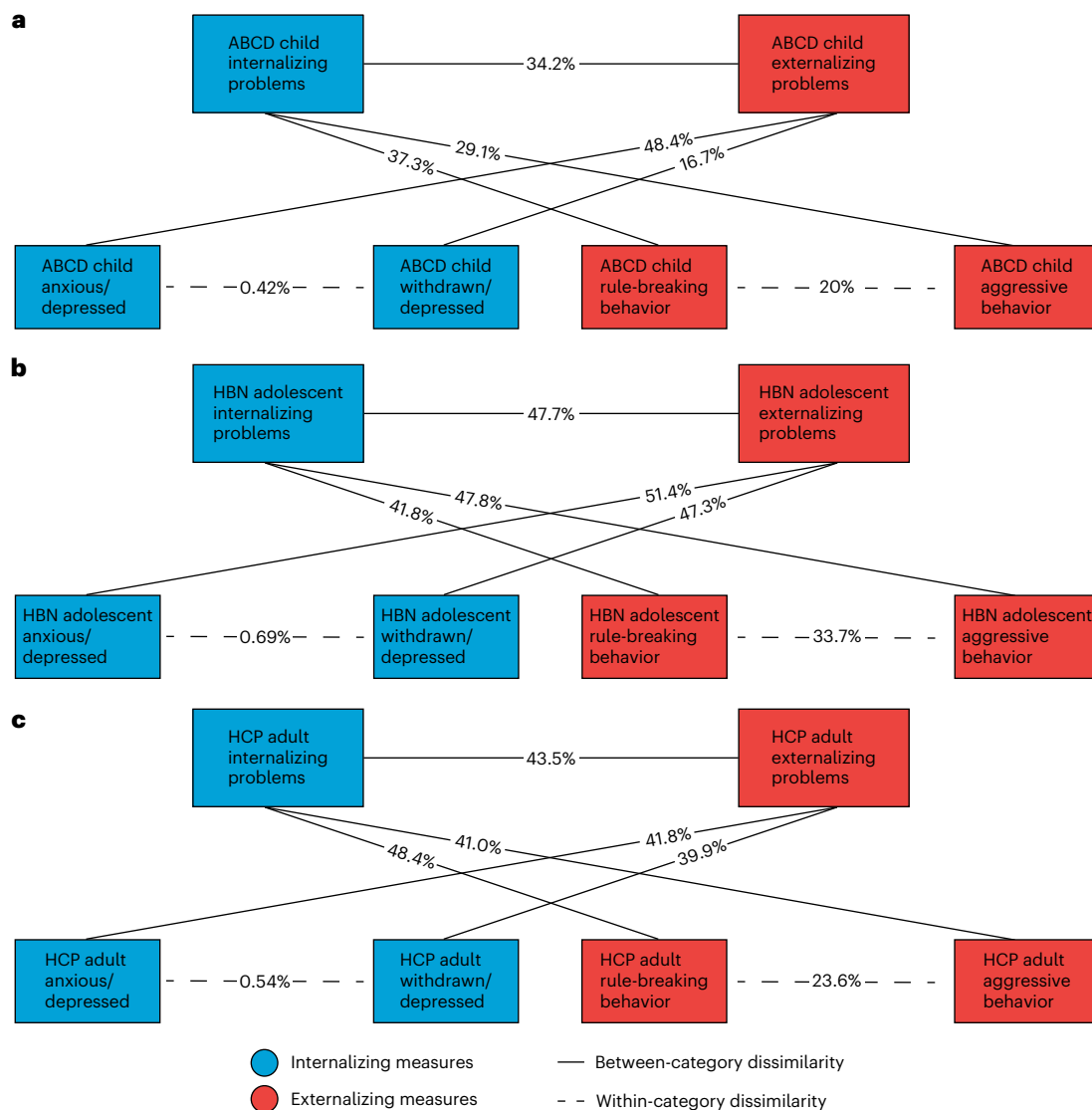


**Fig. 2 | Distinct RSFC features predict internalizing and externalizing behaviors across all samples. a–c.** More similar predictive RSFC features are seen within than between behavioral categories in ABCD children (a), HBN adolescents (b) and HCP adults (c). Numbers reflect the proportion of RSFC

edges at which predictive feature weights associated with a pair of behavioral measures were significantly different according to the two-tailed exact tests of differences after FDR correction ( $q < 0.05$ ).

permutation. Permutation testing was performed on mean predictive feature weights from each of the resulting 171 unique network blocks. Statistically significant predictive feature weights were summed across each row on Fig. 4a and plotted on brain surface on Fig. 4b for the positive weights and on Fig. 4c for the negative weights.

Figure 4 illustrates that both shared and unique RSFC patterns predict total internalizing and externalizing problems among ABCD children, HBN adolescents and HCP adults. To determine which network block(s) drive the prediction of total internalizing and externalizing problems in each sample, we averaged statistically significant predictive feature weights from Fig. 4a across all subnetworks within eight large-scale functional networks—temporal-parietal, default, frontoparietal, limbic, salience/ventral attention, dorsal attention, somato/motor and visual—and within the subcortical regions, resulting in a  $9 \times 9$  matrix of network-level average predictive feature weights for each total score and each sample. We then determined the three network blocks with the most positive and negative average predictive feature weights with respect to each total score and each sample (Supplementary Table 16).

According to exact tests of differences, RSFC edges between the temporal-parietal network and the subcortical predicted total internalizing problems more positively or less negatively than total externalizing problems across all three samples (Supplementary Tables 13–15). These differences seemed to be driven by highly negative predictions of total externalizing problems in both ABCD children and HBN adolescents and by highly positive predictions of total internalizing problems in HCP adults. A similar pattern was observed for the network block involving subcortical regions and the somato/motor network (Supplementary Table 16). These results suggest that decreased FC of the temporal-parietal and somato/motor networks with the subcortical regions may be specific predictors of externalizing behavior across childhood and adolescence, and increased FC within these network blocks may be specific predictors of internalizing behavior in adulthood.

Results from the exact tests of differences also showed that between-network FC involving the visual network predicted total externalizing problems more positively or less negatively than total internalizing problems across ABCD children and HBN adolescents

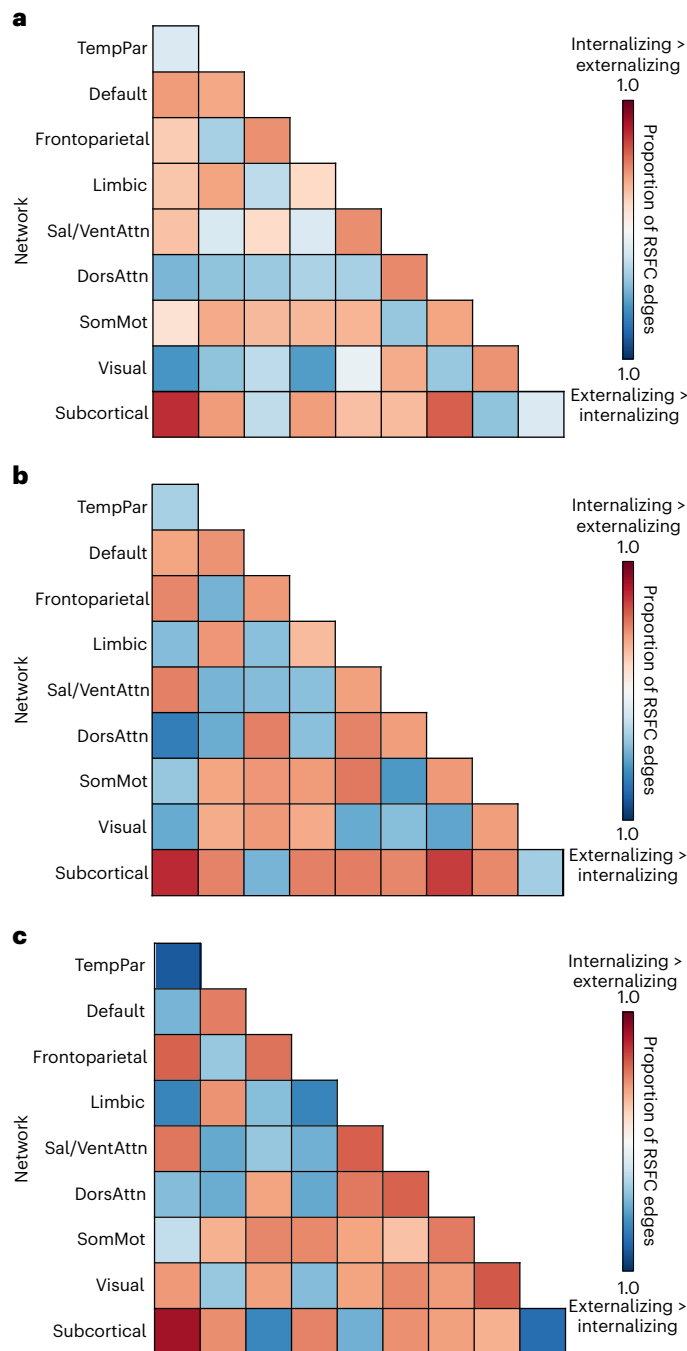


**Fig. 3 | Differential RSFC predictors of internalizing and externalizing behaviors across network blocks within each sample. a–c,** Proportions of RSFC edges at which predictive feature weights are significantly different between total internalizing problems and total externalizing problems within and between large-scale functional networks and subcortical regions in ABCD children (a), HBN adolescents (b) and HCP adults (c). If predictive feature weights associated with total internalizing problems across all RSFC edges within a network block were on average more positive or less negative/more negative or less positive than those associated with total externalizing problems, the network block is red/blue. TempPar, temporal-parietal; Sal/VentAttn, salience/ventral attention; DorsAttn, dorsal attention; SomMot, somato/motor.

(Supplementary Tables 13 and 14). These significant differences were driven by highly negative prediction of total internalizing problems in both samples (Supplementary Table 16), suggesting that decreased between-network FC involving the visual network may be a specific predictor of internalizing behavior in childhood and adolescence.

Finally, RSFC edges within the limbic and temporal-parietal networks and within the subcortical regions predicted total externalizing problems more positively than total internalizing problems among HCP adults (Supplementary Table 15). These three sets of RSFC edges exhibited the most positive predictive feature weights with respect to total externalizing problems in HCP adults (Supplementary Table 16), suggesting that increased FC within the limbic and temporal-parietal networks and within the subcortical region may be specific predictors of externalizing behavior in adulthood.

## Discussion

In this study, we first used RSFC data from a large, diverse sample of children to predict internalizing- and externalizing-related behaviors. Predictive feature weights associated with behavioral pairs within internalizing and externalizing categories were more similar than predictive feature weights between categories. We repeated these analyses in an independent sample of adolescents and young adults and observed the same pattern. These results suggest that functional network predictors of internalizing and externalizing behaviors may be more similar within the same symptom classes than between different symptom classes across distinct developmental stages.

Internalizing and externalizing symptoms reflect distinct factors across various mental disorders, irrespective of demographic and collection method<sup>31–35</sup>. Although large-scale networks can be mechanistically informative for studying neurocognitive processes<sup>36,37</sup> and psychiatric phenotypes<sup>10,38–40</sup>, the similarity of whole-brain RSFC patterns predicting measures of internalizing and externalizing behavior has not been directly assessed. Previous work has shown that predictive network features are similar across behaviors within the broad categories of mental health<sup>11</sup>. Using KRR models<sup>11,41</sup>, we were able to show that beyond this broad pattern of similarity within the general domain of mental health, predictive feature weights were more similar within than between behavioral categories across ABCD children, HBN adolescents and HCP adults. Of note, this cross-sample consistency was robust to differences in demographic characteristics, model implementation, imaging acquisition and processing protocols across cohorts. These findings are consistent with theoretical models that consider internalizing and externalizing behaviors as distinct constructs of psychopathology under a general psychopathology  $p$  factor<sup>28,29</sup>.

We also investigated functional network predictors that differentially predicted total internalizing and externalizing problems in each dataset. Across both ABCD children and HBN adolescents, between-network RSFC edges to the visual network contained more negative feature weights when predicting total internalizing problems than when predicting total externalizing problems and were among the most negative predictors of total internalizing problems. Furthermore, RSFC edges from the other functional networks to the subcortical regions, particularly RSFC from the temporal-parietal and somato/motor networks to the subcortical regions, exhibited more negative feature weights predicting total externalizing problems than total internalizing problems, and were among the most negative predictors of total externalizing problems. By contrast, the same sets of RSFC edges to the subcortical regions exhibited more positive feature weights predicting total internalizing problems than total externalizing problems and were among the most positive predictors of total internalizing problems among HCP adults. Another observation from the HCP adults is that RSFC edges within the limbic and temporal-parietal networks and within the subcortical regions exhibited increased feature weights when predicting total internalizing problems than when predicting total externalizing problems and were among the most positive predictors of total internalizing problems. Broadly, these results suggest that decreased between-network FC involving the visual network may be a specific predictor of internalizing behavior, while decreased FC between temporal-parietal and somato/motor networks and the subcortical regions may be a specific predictor of

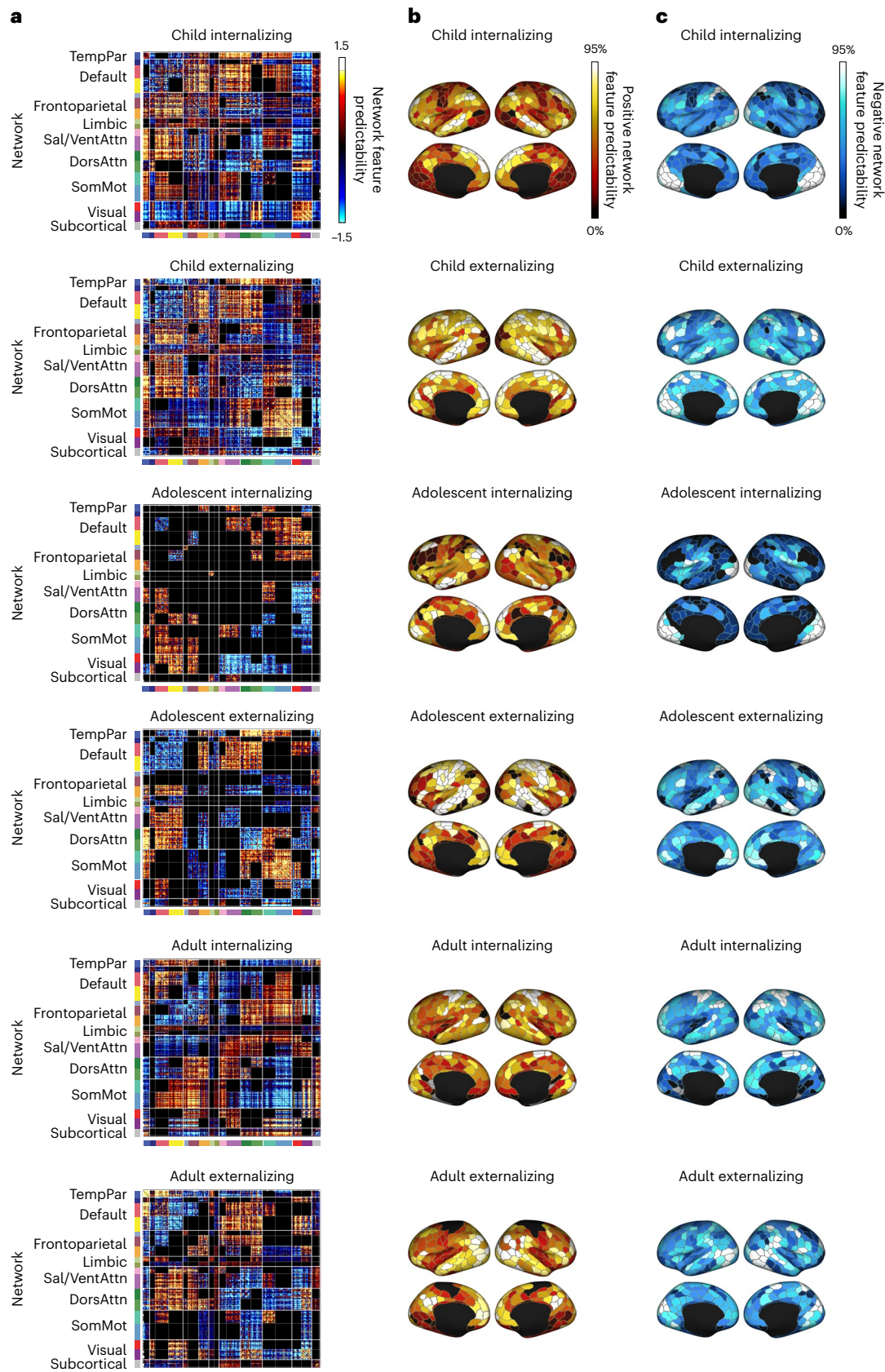


**Fig. 4 | Predictive RSFC feature weights associated with total internalizing problems and total externalizing problems in ABCD children, HBN adolescents and HCP adults. a**, Significant feature weights based on permutation testing within and between large-scale functional networks and subcortical regions **b**, Positive predictive feature weights summed across rows of panel **a** for each cortical region. Here stronger RSFC associated with a given

cortical region predicts higher behavioral scores. **c**, Negative predictive feature weights summed across rows of panel **a** for each cortical region. Here weaker RSFC associated with a given cortical region predicts higher behavioral scores. In both panels **b** and **c**, the color of each cortical region indicates its percentile among 400 regions.

externalizing behavior across childhood and adolescence. Conversely, increased FC within the limbic and temporal-parietal networks and within the subcortical regions may be a specific predictor of externalizing behavior in adulthood.

Our results highlight the importance of FC between the temporal-parietal and somato/motor networks and the subcortical regions in predicting internalizing and externalizing behavior across the three samples. The temporal-parietal network regions are theorized to be important for social emotion processing<sup>42,43</sup> and theory of mind<sup>44,45</sup>, while the somato/motor network encompasses motor processing regions<sup>46–49</sup>. The strengths of their FC with the subcortical regions have been identified as unique correlates of externalizing behavior in preadolescence according to one previous study<sup>50</sup>. Our results partially agreed with this previous finding that while these RSFC metrics may be specific predictors of externalizing behavior in childhood and adolescence, they may become specific predictors of internalizing behavior in adulthood.

Overall, we observed both shared and unique RSFC predictive features associated with internalizing and externalizing behavior across datasets. The differences in predictive feature patterns may be attributable to development of functional network organization from childhood through adolescence and then adulthood<sup>14,15,51–53</sup>, or to site or acquisition differences among the three collection efforts. Of note, our interpretations are limited by the cross-sectional nature of the available data. In addition, many participants were excluded due to image-quality issues (Supplementary Table 1). As such, the resulting sample was not demographically matched across the included and excluded participants. There is a clear tension between previous work indicating that in-scanner motion can result in systematic artifacts in FC<sup>54,55</sup> and that predictive models can fail to generalize across populations<sup>56,57</sup>. In part, this may be addressed through the future availability of longitudinal samples that extend from childhood through adolescence and adulthood, allowing for the direct assessment of longitudinal trajectories of brain development and associated brain-based predictions within individuals across the lifespan. Another limitation of our study is that we did not test our models separately in each sex. Previous studies have suggested brain-based predictive models often fail to generalize across sexes<sup>57</sup>, and future work should test sex-/gender-specific models of behavior<sup>58</sup>. Moreover, behavioral scores of the ABCD children were reported by their parents, and these children's self-reported scores were not available. As such, the difference patterns we observed across samples failed to account for the effects of reporter bias.

Taken together, our study found that predictive network features are more similar within than between categories of internalizing and externalizing behavior across three datasets characterized by distinct developmental stages. Negative RSFC edges from other large-scale networks to the visual network and to the subcortical regions most differentially predicted internalizing and externalizing behavior, respectively, in ABCD children and HBN adolescents. However, increased FC between temporal-parietal and somato/motor networks and the subcortical regions and those within the limbic and temporal-parietal networks as well as the subcortical regions most differentially predicted internalizing and externalizing behavior, respectively, in HCP adults. Future work will benefit from the longitudinal study of common and distinct brain-based predictive features across childhood, adolescence and adulthood.

## Methods

### Participants

A total of 11,875 typically developing children and their parents across 21 sites in the United States participated in the ABCD study at baseline (ABCD release 2.0.1). The ABCD study was approved by the institutional review board at the University of California, San Diego<sup>59</sup>. Parents or guardians provided written consent, while each child provided written assent for participation<sup>60</sup>. The final analytical sample consisted of 5,260

unrelated children ( $M_{\text{age}} = 9.94$ , 48.88% female) who passed strict preprocessing quality control and had complete rsfMRI data and complete scores across all behavioral measures. The percentages of biological mother and father reporters in the final sample are 85.0% and 10.2%, respectively. We combined the 21 ABCD sites into 8 'site categories' to reduce sample size variability across sites (Supplementary Table 2). Participants within the same site were also in the same site category. Detailed demographic information can be found in Supplementary Table 1.

The HBN project was approved by the Chesapeake Institutional Review Board (now Advarra, <https://www.advarra.com/>) and aims to recruit 10,000 individuals aged between 5 and 21 years from the New York area<sup>17</sup>. All participants aged over 18 years provided written informed consent, while all participants aged below 18 years provided written assent along with their legal guardians' written informed consent<sup>17</sup>. After completion of the study, all participants were offered referral information and up to three in-person feedback sessions as well as monetary compensation<sup>17</sup>. Following data processing and quality control, 412 participants aged between 12 and 18 years from the HBN study (HBN releases 1–7 (ref. 17)) were available for analyses. Our final analytical sample consisted of 229 adolescents ( $M_{\text{age}} = 14.73$ , 42.36% female) who did not differ from ABCD children in the levels of total internalizing and total externalizing problems (Supplementary Table 11). Detailed demographic information can be found in Supplementary Table 5.

A total of 1,206 healthy adults participated in the HCP study (HCP S1200 Data Release) and provided written informed consent before participation in the study<sup>18</sup>. After preprocessing quality control of imaging data, participants were filtered from Li's set of 953 participants<sup>61</sup> on the basis of the availability of a complete set of structural fMRI and rsfMRI scans, as well as all behavioral scores of interest. Our main analysis consisted of 423 adult participants ( $M_{\text{age}} = 28.99$ , 56.74% female) who fulfilled all selection criteria<sup>12</sup> and did not differ from ABCD children in the levels of total internalizing and total externalizing problems (Supplementary Table 12). Detailed demographic information can be found in Supplementary Table 8.

### Neuroimaging

**Data acquisition.** For the ABCD study, all T1w images and fMRI data were acquired using protocols harmonized across three Tesla scanner platforms (Phillips, Siemens Prisma and General Electric 750) at 21 sites. Twenty minutes of rsfMRI data, consisting of four 5 min runs, was collected from each ABCD child participant. The structural T1 scans were acquired with 1 mm isotropic resolution with a repetition time (TR) of 2,500 ms. Full details of imaging acquisition can be found elsewhere<sup>62</sup>.

The fMRI data in the HCP data were acquired using an optimized protocol with 2 mm isotropic resolution and a TR of 720 ms. Each HCP participant went through one structural MRI session and two fMRI sessions. Each fMRI session consisted of two 15 min resting-state scans with opposite phase encoding directions (left/right and right/left). The structural T1 scans were acquired using 0.7 mm isotropic resolution and a TR of 2,400 ms. Full details of the acquisition protocol can be found elsewhere<sup>18</sup>.

**Data processing.** Minimally preprocessed T1w images<sup>63</sup> in the ABCD study were further processed using FreeSurfer v.5.3.0<sup>64–69</sup>. The cortical surface meshes were then registered to a common spherical coordinate system<sup>66,67</sup>. Participants who failed recon-all quality control in FreeSurfer were subsequently excluded<sup>63</sup>. The minimally preprocessed fMRI data<sup>63</sup> were subsequently processed in the following manner. The initial frames were removed depending on the type of scanner<sup>63</sup>. The resulting fMRI images were then aligned with the processed T1w images<sup>70</sup> with FsFast<sup>71</sup>, and only runs with registration costs less than 0.6 were retained. Framewise displacement (FD)<sup>72</sup> and voxel-wise differentiated signal variance (DVARs)<sup>55</sup> were computed by `fsl_motion_outliers`.

Volumes with  $FD > 0.3$  mm or  $DVARS > 50$ , along with one volume before and two volumes after, were flagged as outliers. A bandstop filter was applied to remove respiratory pseudomotion (0.31–0.43 Hz)<sup>73</sup>. Uncensored segments of data having fewer than five contiguous volumes were also flagged as outliers and censored<sup>74,75</sup>. Runs with more than half of the volumes flagged as outliers and/or maximum  $FD > 5$  mm were discarded. Participants with less than 4 min of data were excluded from further analysis. Nuisance regressors, including global signal, six motion correction parameters, averaged ventricular signal, averaged white matter signal and their temporal derivatives (18 regressors in total), were regressed out of the fMRI time series from the unflagged volumes. Data were interpolated across censored frames<sup>76</sup>, band-pass filtered at  $0.009 \text{ Hz} \leq f \leq 0.080 \text{ Hz}$ , projected onto FreeSurfer fsaverage6 surface space and smoothed using a 6 mm full-width half maximum kernel.

The rsfMRI data from the HBN dataset were preprocessed with the following steps: (1) removal of the first eight frames; (2) slice time correction; (3) motion correction and outlier detection: frames with  $FD > 0.3$  mm or  $DVARS > 60$  were flagged as censored frames; one frame before and two frames after these volumes were flagged as censored frames; uncensored segments of data lasting fewer than five contiguous frames were also labeled as censored frames<sup>74,75</sup>; blood-oxygen-level dependent runs with over half of the frames censored and runs with maximum  $FD > 5$  mm were removed; (4) correction for susceptibility induced spatial distortion; (5) alignment with structural image using boundary-based registration<sup>70</sup>; (6) nuisance regression: regressed out a vector of ones and linear trend, global signal, six motion correction parameters, averaged ventricular signal, averaged white matter signal and their temporal derivatives; regression coefficients were estimated from the non-censored volumes; (7) band-pass filtering ( $0.009 \text{ Hz} \leq f \leq 0.080 \text{ Hz}$ ); (8) interpolation of censored frames; (9) projection onto the FreeSurfer fsaverage6 surface space; (10) smoothing with 2 mm full-width half maximum and down-sampling to fsaverage5 surface space. Since the HBN dataset involved three different sites, we harmonized the rsfMRI data using the neuroCombat package in R<sup>77</sup>.

For the HCP study, minimally preprocessed T1w images<sup>78</sup> went through bias and distortion correction using the PreFreeSurfer pipeline and registered to MNI space. Cortical surface reconstruction was conducted using FreeSurfer v.5.2 using recon-all adapted for high-resolution images. The reconstructed surface meshes were then registered to the Conte69 surface template<sup>79</sup>. During fMRI preprocessing, the fMRI data were first corrected for gradient-nonlinearity-induced distortions. The fMRI time series in each frame were then realigned to the single-band reference image to correct for subject motion using rigid body transformation<sup>72,80</sup> with the FMRIB Software Library (FSL)<sup>81</sup>. The resulting single-band image underwent spline interpolation to correct for distortions and was then registered to the T1w image<sup>70</sup>. The registered fMRI volumes then went through nonlinear registration to the Conte69 surface template<sup>79</sup> and mapped to the standard CIFTI (Connectivity Informatics Technology Initiative) grayordinate coordinate space. Further details about the preprocessing and processing pipelines of structural and functional images can be found elsewhere<sup>78</sup>.

**Functional connectivity.** We defined 400 cortical ROIs<sup>22</sup> and 19 subcortical ROIs<sup>23</sup> for each sample. FC was measured by Pearson's  $r$  correlations between the mean time series of each pair of ROIs. Censored frames were ignored when computing FC. The average FC matrix across all runs in each participant was computed and used for subsequent analyses.

### Measures of internalizing and externalizing behaviors

We included six measures of internalizing and externalizing behavior in our analyses, selected from the Achenbach Child Behavior Checklist (CBCL)<sup>20</sup> taken from child participants<sup>82</sup> in the ABCD study. We then

assigned three measures to the child internalizing category (Total Child Internalizing Problems, Child Anxious/Depressed, Child Withdrawn/Depressed) and the other three measures to the child externalizing category (Total Child Externalizing Problems, Child Rule-Breaking Behavior, Child Aggressive Behavior; Supplementary Table 4). The Total Child Internalizing Problems Scale is the sum of the Anxious/Depressed, Withdrawn/Depressed and Somatic Complaints Syndrome Subscales from the CBCL<sup>20</sup>. The Total Child Externalizing Problems Scale is the sum of the Rule-Breaking Behavior and the Aggressive Behavior Syndrome Subscales from the CBCL<sup>20</sup>. Participants without available data across all behavioral measures were excluded from analysis.

In the HBN sample, we analyzed the same CBCL measures as in the ABCD sample (Supplementary Table 6) and assigned the same sets of measures to adolescent internalizing and externalizing categories (Supplementary Table 7). Similarly, the Total Adolescent Internalizing Problems Scale is the sum of the Anxious/Depressed, Withdrawn/Depressed and Somatic Complaints Syndrome Subscales from the CBCL<sup>20</sup>. The Total Adolescent Externalizing Problems Scale is the sum of the two subscales under the adolescent externalizing category<sup>20</sup>.

In the HCP dataset, we analyzed six measures of internalizing and externalizing behaviors from the Achenbach Self-Report (ASR) questionnaire<sup>21</sup> (Supplementary Table 9). These subscales assess a corresponding set of symptoms to the CBCL subscales in the ABCD sample. We assigned three measures (Total Adult Internalizing Problems, Adult Anxious/Depressed, Adult Withdrawn) to the adult internalizing category and the other three (Total Adult Externalizing Problems, Adult Rule-Breaking Behavior, Adult Aggressive Behavior) to the adult externalizing category (Supplementary Table 10). The Total Adult Internalizing Problems Scale is the sum of the Anxious/Depressed, Withdrawn and Somatic Complaints Syndrome Subscales from the ASR<sup>21</sup>. The Total Adult Externalizing Problems Scale is the sum of Rule-Breaking and Aggressive Behavior Syndrome Subscales from the ASR<sup>21</sup>.

### Statistical analysis

Consistent with previous work<sup>11</sup>, we used KRR with  $l_2$  regularization to predict each behavioral measure from participant-specific RSFC matrices in each of the three samples. Details about the KRR model can be found in Supplementary Methods 1). Age and sex were entered as covariates. The KRR model assumes that participants with more similar FC patterns have more similar behavioral measures and was implemented with nested cross-validation procedures similar to those of ref. 12.

In the ABCD analyses, we performed leave-three-site-clusters-out nested cross-validation for each behavioral measure. At each fold, a different set of three site categories served as the test set, and the remaining five site categories were used as the training set, resulting in 56 folds in total. Participants from the same site were all in either the training set or the testing set. In the HBN and HCP analyses, we implemented 60 random initiations of tenfold nested cross-validation. Participants from the same family were assigned to either training or testing sets and were never split across training and test sets in any cross-validation fold.

Across all samples, model and regularization parameters were estimated from the training set at each fold. The estimated parameters were then applied to the unseen participants from the test set and evaluated for accuracy by correlating predicted and actual measures<sup>83</sup>. To assess whether model prediction performed better than chance, statistical significance of prediction accuracy was assessed by a permutation test whereby the entire cross-validation procedure was rerun on behavior measures randomly reshuffled across participants in each dataset. This generated a null distribution where a participant's RSFC data were used to predict the measure of another participant from the same site, and the resulting null distribution would capture within-site similarity. Care was taken to avoid shuffling between families or sites.

## Model interpretation

To interpret the predictive importance of each RSFC feature, we used an approach from Haufe and colleagues<sup>25</sup> to transform predictive feature weights associating each RSFC edge with the behavioral measure. Predictive feature weight was computed by the covariance between the predicted behavioral measure and the RSFC edge. This resulted in a  $419 \times 419$  predictive feature matrix for each behavioral measure. A positive (or negative) predictive feature weight indicates that higher RSFC predicts greater (or lower) behavioral values. Statistical significance of these predictive feature weights was tested with permutation tests and corrected for multiple comparison using FDR ( $q < 0.05$ ). To reduce the number of multiple comparisons, predictive feature weights were averaged within and between 18 large-scale functional networks<sup>22,23</sup> before conducting the permutation test.

To compare predictive network patterns within and between internalizing and externalizing behaviors, we conducted exact tests of differences<sup>19</sup> between pairs of Haufe-transformed<sup>25</sup> weight vectors associated with each RSFC edge predicting different pairs of behavioral measures across all cross-validation folds. If predictive feature weight values associated with an RSFC edge predicting one behavioral measure are either larger or smaller than those associated with the same edge predicting the other behavioral measure across more than 97.5% of all cross-validation folds, the two-tailed  $P$  value would be smaller than 0.05, and the predictive feature weights associated with the two measures would be considered significantly different from each other. When comparing between each pair of behavioral measures, we repeated the exact test of differences across all 87,571 RSFC edges and corrected for multiple comparisons using FDR. Finally, we determined the proportion of edges at which the exact test of differences remained statistically significant after FDR for each behavioral comparison.

We conducted exact tests of difference between predictive feature weights associated with the following pairs of behavioral measures that were found in both CBCL and ASR questionnaires (see Supplementary Tables 1 and 2 for category assignment): Anxious/Depressed Syndrome Subscale and Withdrawn/Depressed Syndrome Subscale, Rule-Breaking Behavior Syndrome Subscale and Aggressive Behavior Syndrome Subscale, Anxious/Depressed Syndrome Subscale and Total Externalizing Problems Scale, Withdrawn Syndrome Subscale and Total Externalizing Problems, Rule-Breaking Behavior Syndrome Subscale and Total Internalizing Problems Scale, Aggressive Behavior Syndrome Subscale and Total Internalizing Problems Scale, Total Internalizing Problems Scale and Total Externalizing Problems Scale.

## Reporting summary

Further information on research design is available in the Nature Portfolio Reporting Summary linked to this article.

## Data availability

The ABCD data are publicly available via the NIMH Data Archive (NDA) and via <https://abcdstudy.org>. The HBN data are publicly available via Child Mind Institute Healthy Brain Network at [http://fcon\\_1000.projects.nitrc.org/indi/cmi\\_healthy\\_brain\\_network/Data.html](http://fcon_1000.projects.nitrc.org/indi/cmi_healthy_brain_network/Data.html). The HCP data are also publicly available and can be accessed via <https://www.humanconnectome.org>. Access to all three datasets requires Data Use Agreement.

## Code availability

Code for this study is publicly available via Github under the main branch: <https://github.com/quyueyue/InternalizingExternalizingPredictions.git>. The software dependencies were Freesurfer (5.3.0; <https://surfer.nmr.mgh.harvard.edu>), FSL (5.0.8; <https://fsl.fmrib.ox.ac.uk/fsl/fslwiki/FslInstallation>), MATLAB (2018b; <https://www.mathworks.com/products/matlab.html>), Jupyter Notebook 6.4.5 (Python 3.9.7 ipykernel; <https://jupyter.org>), Python/3.10.8-GCCcore-12.2.0 (<https://www.python.org>) and the neuroCombat (v.1.0.13) package in R v.4.2.0.

## References

- Achenbach, T. M. The child behavior profile: I. Boys aged 6–11. *J. Consult. Clin. Psychol.* **46**, 478–488 (1978).
- Achenbach, T. M. *Manual for the Child Behavior Checklist/ 4–18 and 1991 Profile* (Univ. Vermont, Department of Psychiatry, 1991).
- Duprey, E. B., Oshri, A. & Liu, S. Developmental pathways from child maltreatment to adolescent suicide-related behaviors: the internalizing and externalizing comorbidity hypothesis. *Dev. Psychopathol.* **32**, 945–959 (2020).
- Commissio, M. et al. Childhood externalizing, internalizing and comorbid problems: distinguishing young adults who think about suicide from those who attempt suicide. *Psychol. Med.* <https://doi.org/10.1017/S0033291721002464> (2021).
- Papachristou, E. & Flouri, E. The codevelopment of internalizing symptoms, externalizing symptoms, and cognitive ability across childhood and adolescence. *Dev. Psychopathol.* **32**, 1375–1389 (2020).
- Narusyte, J., Ropponen, A., Alexanderson, K. & Svedberg, P. Internalizing and externalizing problems in childhood and adolescence as predictors of work incapacity in young adulthood. *Soc. Psychiatry Psychiatr. Epidemiol.* **52**, 1159 (2017).
- Sripada, C. et al. Prediction of neurocognition in youth from resting state fMRI. *Mol. Psychiatry* **25**, 3413–3421 (2019).
- Shannon, B. J. et al. Premotor functional connectivity predicts impulsivity in juvenile offenders. *Proc. Natl Acad. Sci. USA* **108**, 11241–11245 (2011).
- Uddin, L. Q. et al. Salience network-based classification and prediction of symptom severity in children with autism. *JAMA Psychiatry* **70**, 869 (2013).
- Lake, E. M. R. et al. The functional brain organization of an individual allows prediction of measures of social abilities transdiagnostically in autism and attention-deficit/hyperactivity disorder. *Biol. Psychiatry* **86**, 315–326 (2019).
- Chen, J. et al. Shared and unique brain network features predict cognitive, personality, and mental health scores in the ABCD study. *Nat. Commun.* **13**, 2217 (2022).
- Ooi, L. Q. R. et al. Comparison of individualized behavioral predictions across anatomical, diffusion and functional connectivity MRI. *Neuroimage* **263**, 119636 (2022).
- Sydnor, V. J. et al. Neurodevelopment of the association cortices: patterns, mechanisms, and implications for psychopathology. *Neuron* **109**, 2820–2846 (2021).
- Hwang, K., Hallquist, M. N. & Luna, B. The development of hub architecture in the human functional brain network. *Cereb. Cortex* **23**, 2380–2393 (2013).
- Dong, H. M., Margulies, D. S., Zuo, X. N. & Holmes, A. J. Shifting gradients of macroscale cortical organization mark the transition from childhood to adolescence. *Proc. Natl Acad. Sci. USA* **118**, e2024448118 (2021).
- Volkow, N. D. et al. The conception of the ABCD study: from substance use to a broad NIH collaboration. *Dev. Cogn. Neurosci.* **32**, 4–7 (2018).
- Alexander, L. M. et al. An open resource for transdiagnostic research in pediatric mental health and learning disorders. *Sci. Data* **4**, 170181 (2017).
- Van Essen, D. C. et al. The WU-minn human connectome project: An overview. *Neuroimage* **80**, 62 (2013).
- Mackinnon, J. G. in *Handbook of Computational Econometrics* (eds Belsley, D. A. & Kontoghiorghes, E. J.) 183–213 (Wiley, 2009); <https://doi.org/10.1002/9780470748916.CH6>
- Achenbach, T. M. & Rescorla, L. A. *Manual for ASEBA School-Age Forms & Profiles* (ASEBA, 2001).
- Achenbach, T. M. & Rescorla, L. A. *Manual for the ASEBA Adult Forms & Profiles* (ASEBA, 2003).

22. Schaefer, A. et al. Local-global parcellation of the human cerebral cortex from intrinsic functional connectivity MRI. *Cereb. Cortex* **28**, 3095–3114 (2018).
23. Fischl, B. et al. Whole brain segmentation: automated labeling of neuroanatomical structures in the human brain. *Neuron* **33**, 341–355 (2002).
24. Marek, S. et al. Reproducible brain-wide association studies require thousands of individuals. *Nature* **603**, 654–660 (2022).
25. Haufe, S. et al. On the interpretation of weight vectors of linear models in multivariate neuroimaging. *Neuroimage* **87**, 96–110 (2014).
26. Dhamala, E., Jamison, K. W., Jaywant, A. & Kuceyeski, A. Shared functional connections within and between cortical networks predict cognitive abilities in adult males and females. *Hum. Brain Mapp.* **43**, 1087–1102 (2022).
27. Parkes, L. et al. Transdiagnostic dimensions of psychopathology explain individuals' unique deviations from normative neurodevelopment in brain structure. *Transl. Psychiatry* **11**, 232 (2021).
28. Brislin, S. J. et al. Differentiated nomological networks of internalizing, externalizing, and the general factor of psychopathology (*p* factor) in emerging adolescence in the ABCD study. *Psychol. Med.* **52**, 3051–3061 (2022).
29. Caspi, A. et al. The *p* factor: one general psychopathology factor in the structure of psychiatric disorders? *Clin. Psychol. Sci.* **2**, 119 (2014).
30. Yeo, B. T. T. et al. The organization of the human cerebral cortex estimated by intrinsic functional connectivity. *J. Neurophysiol.* **106**, 1125–1165 (2011).
31. Krueger, R. F., Markon, K. E., Patrick, C. J., Benning, S. D. & Kramer, M. D. Linking antisocial behavior, substance use, and personality: an integrative quantitative model of the adult externalizing spectrum. *J. Abnorm. Psychol.* **116**, 645–666 (2007).
32. Eaton, N. R. et al. An invariant dimensional liability model of gender differences in mental disorder prevalence: evidence from a national sample. *J. Abnorm. Psychol.* **121**, 282–288 (2012).
33. Achenbach, T. M. & Edelbrock, C. S. Psychopathology of childhood. *Annu. Rev. Psychol.* **35**, 227–256 (2003).
34. Kessler, R. C. et al. Development of lifetime comorbidity in the world health organization world mental health surveys. *Arch. Gen. Psychiatry* **68**, 90–100 (2011).
35. Ringwald, W. R., Forbes, M. K. & Wright, A. G. C. Meta-analytic tests of measurement invariance of internalizing and externalizing psychopathology across common methodological characteristics. *J. Psychopathol. Clin. Sci.* **131**, 847–856 (2022).
36. Rosenberg, M. D., Finn, E. S., Scheinost, D., Constable, R. T. & Chun, M. M. Characterizing attention with predictive network models. *Trends Cogn. Sci.* **21**, 290–302 (2017).
37. Rosenberg, M. D. et al. A neuromarker of sustained attention from whole-brain functional connectivity. *Nat. Neurosci.* **19**, 165–171 (2015).
38. Satterthwaite, T. D. et al. Connectome-wide network analysis of youth with psychosis-spectrum symptoms. *Mol. Psychiatry* **20**, 1508–1515 (2015).
39. Pornpattananangkul, N., Leibenluft, E., Pine, D. S. & Stringaris, A. Association between childhood anhedonia and alterations in large-scale resting-state networks and task-evoked activation. *JAMA Psychiatry* **76**, 624–633 (2019).
40. Karcher, N. R., O'Brien, K. J., Kandala, S. & Barch, D. M. Resting-state functional connectivity and psychotic-like experiences in childhood: results from the adolescent brain cognitive development study. *Biol. Psychiatry* **86**, 7–15 (2019).
41. He, T. et al. Deep neural networks and kernel regression achieve comparable accuracies for functional connectivity prediction of behavior and demographics. *Neuroimage* **206**, 116276 (2020).
42. Narumoto, J., Okada, T., Sadato, N., Fukui, K. & Yonekura, Y. Attention to emotion modulates fMRI activity in human right superior temporal sulcus. *Cogn. Brain Res.* **12**, 225–231 (2001).
43. Mellem, M. S., Jasmin, K. M., Peng, C. & Martin, A. Sentence processing in anterior superior temporal cortex shows a social-emotional bias. *Neuropsychologia* **89**, 217–224 (2016).
44. Völlm, B. A. et al. Neuronal correlates of theory of mind and empathy: a functional magnetic resonance imaging study in a nonverbal task. *Neuroimage* **29**, 90–98 (2006).
45. Bigler, E. D. et al. Superior temporal gyrus, language function, and autism. *Dev. Neuropsychol.* **31**, 217–238 (2007).
46. Weinrich, M., Wise, S. P. & Mauritz, K. H. A neurophysiological study of the premotor cortex in the rhesus monkey. *Brain* **107**, 385–414 (1984).
47. Cunnington, R., Windischberger, C., Deecke, L. & Moser, E. The preparation and readiness for voluntary movement: a high-field event-related fMRI study of the Bereitschafts-BOLD response. *Neuroimage* **20**, 404–412 (2003).
48. Kwan, H. C., MacKay, W. A., Murphy, J. T. & Wong, Y. C. Spatial organization of precentral cortex in awake primates. II. Motor outputs. *J. Neurophysiol.* **41**, 1120–1131 (1978).
49. Penfield, W. & Boldrey, E. Somatic motor and sensory representation in the cerebral cortex of man as studied by electrical stimulation. *Brain* **60**, 389–443 (1937).
50. Lees, B. et al. Altered neurocognitive functional connectivity and activation patterns underlie psychopathology in preadolescence. *Biol. Psychiatry Cogn. Neurosci. Neuroimaging* **6**, 387–398 (2021).
51. Grayson, D. S. & Fair, D. A. Development of large-scale functional networks from birth to adulthood: a guide to neuroimaging literature. *Neuroimage* **160**, 15 (2017).
52. Galván, A. & Tottenham, N. in *Developmental Psychopathology* 3rd edn (ed. Cicchetti, D.) Ch. 18 (Wiley, 2016); <https://doi.org/10.1002/9781119125556.DEVPSY218>
53. Casey, B. J., Galván, A. & Somerville, L. H. Beyond simple models of adolescence to an integrated circuit-based account: a commentary. *Dev. Cogn. Neurosci.* **17**, 128 (2016).
54. van Dijk, K. R. A., Sabuncu, M. R. & Buckner, R. L. The influence of head motion on intrinsic functional connectivity MRI. *Neuroimage* **59**, 431 (2012).
55. Power, J. D., Barnes, K. A., Snyder, A. Z., Schlaggar, B. L. & Petersen, S. E. Spurious but systematic correlations in functional connectivity MRI networks arise from subject motion. *Neuroimage* **59**, 2142–2154 (2012).
56. Li, J. et al. Cross-ethnicity/race generalization failure of behavioral prediction from resting-state functional connectivity. *Sci. Adv.* **8**, 1812 (2022).
57. Dhamala, E., Yeo, B. T. T. & Holmes, A. J. One size does not fit all: methodological considerations for brain-based predictive modeling in psychiatry. *Biol. Psychiatry* **93**, 717–728 (2023).
58. Dhamala, E. et al. Brain-based predictions of psychiatric illness-linked behaviors across the sexes. *Biol. Psychiatry* <https://doi.org/10.1016/J.BIOPSYCH.2023.03.025> (2023).
59. Aucter, A. M. et al. A description of the ABCD organizational structure and communication framework. *Dev. Cogn. Neurosci.* **32**, 8–15 (2018).
60. Clark, D. B. et al. Biomedical ethics and clinical oversight in multisite observational neuroimaging studies with children and adolescents: the ABCD experience. *Dev. Cogn. Neurosci.* **32**, 143–154 (2018).
61. Li, J. et al. Global signal regression strengthens association between resting-state functional connectivity and behavior. *Neuroimage* **196**, 126–141 (2019).
62. Casey, B. J. et al. The Adolescent Brain Cognitive Development (ABCD) study: imaging acquisition across 21 sites. *Dev. Cogn. Neurosci.* **32**, 43 (2018).

63. Hagler, D. J. et al. Image processing and analysis methods for the Adolescent Brain Cognitive Development Study. *Neuroimage* **202**, 116091 (2019).
64. Fischl, B., Liu, A. & Dale, A. M. Automated manifold surgery: constructing geometrically accurate and topologically correct models of the human cerebral cortex. *IEEE Trans. Med. Imaging* **20**, 70–80 (2001).
65. Dale, A. M., Fischl, B. & Sereno, M. I. Cortical surface-based analysis. I. Segmentation and surface reconstruction. *Neuroimage* **9**, 179–194 (1999).
66. Fischl, B., Sereno, M. I., Tootell, R. B. H. & Dale, A. M. High-resolution intersubject averaging and a coordinate system for the cortical surface. *Hum. Brain Mapp.* **8**, 272 (1999).
67. Fischl, B., Sereno, M. I. & Dale, A. M. Cortical surface-based analysis. II: inflation, flattening, and a surface-based coordinate system. *Neuroimage* **9**, 195–207 (1999).
68. Ségonne, F. et al. A hybrid approach to the skull stripping problem in MRI. *Neuroimage* **22**, 1060–1075 (2004).
69. Ségonne, F., Pacheco, J. & Fischl, B. Geometrically accurate topology-correction of cortical surfaces using nonseparating loops. *IEEE Trans. Med. Imaging* **26**, 518–529 (2007).
70. Greve, D. N. & Fischl, B. Accurate and robust brain image alignment using boundary-based registration. *Neuroimage* **48**, 63 (2009).
71. *FsFast - Free Surfer wiki*. <https://surfer.nmr.mgh.harvard.edu/fswiki/FsFast> (2011).
72. Jenkinson, M., Bannister, P., Brady, M. & Smith, S. Improved optimization for the robust and accurate linear registration and motion correction of brain images. *Neuroimage* **17**, 825–841 (2002).
73. Gratton, C. et al. Removal of high frequency contamination from motion estimates in single-band fMRI saves data without biasing functional connectivity. *Neuroimage* **217**, 116866 (2020).
74. Gordon, E. M. et al. Generation and evaluation of a cortical area parcellation from resting-state correlations. *Cereb. Cortex* **26**, 288–303 (2016).
75. Kong, R. et al. Spatial topography of individual-specific cortical networks predicts human cognition, personality, and emotion. *Cereb. Cortex* **29**, 2533–2551 (2019).
76. Power, J. D. et al. Methods to detect, characterize, and remove motion artifact in resting state fMRI. *Neuroimage* **84**, 320–341 (2014).
77. Yu, M. et al. Statistical harmonization corrects site effects in functional connectivity measurements from multi-site fMRI data. *Hum. Brain Mapp.* **39**, 4213 (2018).
78. Glasser, M. F. et al. The minimal preprocessing pipelines for the Human Connectome Project. *Neuroimage* **80**, 105–124 (2013).
79. Van Essen, D. C., Glasser, M. F., Dierker, D. L., Harwell, J. & Coalson, T. Parcellations and hemispheric asymmetries of human cerebral cortex analyzed on surface-based atlases. *Cereb. Cortex* **22**, 2241–2262 (2012).
80. Jenkinson, M. & Smith, S. A global optimisation method for robust affine registration of brain images. *Med. Image Anal.* **5**, 143–156 (2001).
81. Smith, S. M. et al. Advances in functional and structural MR image analysis and implementation as FSL. *Neuroimage* **23**, S208–S219 (2004).
82. Barch, D. M. et al. Demographic, physical and mental health assessments in the adolescent brain and cognitive development study: rationale and description. *Dev. Cogn. Neurosci.* **32**, 55–66 (2018).
83. Finn, E. S. et al. Functional connectome fingerprinting: identifying individuals using patterns of brain connectivity. *Nat. Neurosci.* **18**, 1664–1671 (2015).
84. Kong, R. Schaefer2018 parcellation 400-region 17-network in fsr space. *Figshare* <https://doi.org/10.6084/m9.figshare.10062482.v1> (2019).
85. Orban, C. Subcortical\_regions.png. *Figshare* <https://doi.org/10.6084/m9.figshare.10063016.v1> (2019).

## Acknowledgments

Data used in the preparation of this article were obtained, in part, from the Adolescent Brain Cognitive Development (ABCD) Study (<https://abcdstudy.org>), held in the NIMH Data Archive (NDA). This is a multisite, longitudinal study designed to recruit more than 10,000 children aged 9–10 and follow them over 10 years into early HCP adults. The ABCD study is supported by the National Institutes of Health and additional federal partners under award numbers U01DA041048, U01DA050989, U01DA051016, U01DA041022, U01DA051018, U01DA051037, U01DA050987, U01DA041174, U01DA041106, U01DA041117, U01DA041028, U01DA041134, U01DA050988, U01DA051039, U01DA041156, U01DA041025, U01DA041120, U01DA051038, U01DA041148, U01DA041093, U01DA041089, U24DA041123 and U24DA041147. A full list of supporters is available at [abcdstudy.org/federal-partners.html](http://abcdstudy.org/federal-partners.html). A list of participating sites and a complete list of the study investigators can be found at [abcdstudy.org/consortium\\_members/](http://abcdstudy.org/consortium_members/). ABCD consortium investigators designed and implemented the study and/or provided data but did not necessarily participate in the analysis or writing of this report. Additional data were provided, in part, by the Human Connectome Project, WU-Minn Consortium (Principal Investigators: D. Van Essen and K. Ugurbil; 1U54MH091657) funded by the 16 NIH institutes and centers that support the NIH Blueprint for Neuroscience Research and by the McDonnell Center for Systems Neuroscience at Washington University. This manuscript reflects the views of the authors and may not reflect the opinions or views of the NIH or the ABCD and HCP consortia investigators. This work was supported by the National Institute of Mental Health (R01MH120080 and R01MH123245 to A.J.H.). This work was also supported by the following awards to B.T.T.Y.: NUS Yong Loo Lin School of Medicine (NUHSRO/2020/124/TMR/LOA), the Singapore National Medical Research Council (NMRC) LCG (OFLCG19May-0035), NMRC CTG-IIT (CTGIIT23jan-0001), NMRC STaR (STaR20nov-0003), Singapore Ministry of Health (MOH) Centre Grant (CG21APR1009) and the Temasek Foundation (TF2223-IMH-01). This work was also supported by the following awards to E.D.: the Kavli Institute for Neuroscience at Yale University (Postdoctoral Fellowship for Academic Diversity), the Feinstein Institutes for Medical Research Advancing Women in Science and Medicine (Career Development Award and Barbara Zucker Emerging Scientist Award). Any opinions, findings and conclusions or recommendations expressed in this material are those of the authors and do not reflect the views of the funders. An earlier version of this paper is available at BioRxiv (<https://doi.org/10.1101/2023.05.20.541490v1>).

## Author contributions

Y.L.Q. and A.J.H. designed the research, analyzed and interpreted the results, made figures and wrote the paper. Y.L.Q. conducted the research, analyzed the data and reviewed and published the code. Y.L.Q., J.C., A.T., L.Q.R.O., E.D., C.V.C., S.Z., T.Z., C.L., B.T.T.Y. and A.J.H. provided analytic support. Y.L.Q., J.C., A.T., L.Q.R.O., E.D., C.V.C., S.Z., T.Z., C.L., B.T.T.Y. and A.J.H. edited the paper.

## Competing interests

The authors declare no conflicts of interest.

## Additional information

**Supplementary information** The online version contains supplementary material available at <https://doi.org/10.1038/s44220-025-00388-5>.

**Correspondence and requests for materials** should be addressed to Yueyue Lydia Qu or Avram J. Holmes.

**Peer review information** *Nature Mental Health* thanks Kelley Gunther, Adrienne Romer and the other, anonymous, reviewer(s) for their contribution to the peer review of this work.

**Reprints and permissions information** is available at [www.nature.com/reprints](http://www.nature.com/reprints).

**Publisher's note** Springer Nature remains neutral with regard to jurisdictional claims in published maps and institutional affiliations.

Springer Nature or its licensor (e.g. a society or other partner) holds exclusive rights to this article under a publishing agreement with the author(s) or other rightsholder(s); author self-archiving of the accepted manuscript version of this article is solely governed by the terms of such publishing agreement and applicable law.

© The Author(s), under exclusive licence to Springer Nature America, Inc. 2025

## Reporting Summary

Nature Portfolio wishes to improve the reproducibility of the work that we publish. This form provides structure for consistency and transparency in reporting. For further information on Nature Portfolio policies, see our [Editorial Policies](#) and the [Editorial Policy Checklist](#).

### Statistics

For all statistical analyses, confirm that the following items are present in the figure legend, table legend, main text, or Methods section.

- | n/a                                 | Confirmed                           |  |
|-------------------------------------|-------------------------------------|--|
| <input type="checkbox"/>            | <input checked="" type="checkbox"/> | The exact sample size ( $n$ ) for each experimental group/condition, given as a discrete number and unit of measurement  |
| <input type="checkbox"/>            | <input checked="" type="checkbox"/> | A statement on whether measurements were taken from distinct samples or whether the same sample was measured repeatedly  |
| <input type="checkbox"/>            | <input checked="" type="checkbox"/> | The statistical test(s) used AND whether they are one- or two-sided<br><i>Only common tests should be described solely by name; describe more complex techniques in the Methods section.</i>   |
| <input type="checkbox"/>            | <input checked="" type="checkbox"/> | A description of all covariates tested   |
| <input type="checkbox"/>            | <input checked="" type="checkbox"/> | A description of any assumptions or corrections, such as tests of normality and adjustment for multiple comparisons  |
| <input checked="" type="checkbox"/> | <input type="checkbox"/>            | A full description of the statistical parameters including central tendency (e.g. means) or other basic estimates (e.g. regression coefficient) AND variation (e.g. standard deviation) or associated estimates of uncertainty (e.g. confidence intervals) |
| <input type="checkbox"/>            | <input checked="" type="checkbox"/> | For null hypothesis testing, the test statistic (e.g. $F$ , $t$ , $r$ ) with confidence intervals, effect sizes, degrees of freedom and $P$ value noted<br><i>Give <math>P</math> values as exact values whenever suitable.</i>                            |
| <input checked="" type="checkbox"/> | <input type="checkbox"/>            | For Bayesian analysis, information on the choice of priors and Markov chain Monte Carlo settings   |
| <input checked="" type="checkbox"/> | <input type="checkbox"/>            | For hierarchical and complex designs, identification of the appropriate level for tests and full reporting of outcomes   |
| <input type="checkbox"/>            | <input checked="" type="checkbox"/> | Estimates of effect sizes (e.g. Cohen's $d$ , Pearson's $r$ ), indicating how they were calculated   |

*Our web collection on [statistics for biologists](#) contains articles on many of the points above.*

### Software and code

Policy information about [availability of computer code](#)

Data collection	No software used for data collection.
Data analysis	<p>Custom code for our analyses is publicly available at the following URL:  <a href="https://github.com/quyueyue/InternalizingExternalizingPredictions/tree/main">https://github.com/quyueyue/InternalizingExternalizingPredictions/tree/main</a></p> <p>The following software was used:            MATLAB R2018b (<a href="https://www.mathworks.com/products/matlab.html">https://www.mathworks.com/products/matlab.html</a>)            Freesurfer 5.3.0 (<a href="https://surfer.nmr.mgh.harvard.edu">https://surfer.nmr.mgh.harvard.edu</a>)            FSL 5.0.8 (<a href="https://fsl.fmrib.ox.ac.uk/fsl/fslwiki/FslInstallation">https://fsl.fmrib.ox.ac.uk/fsl/fslwiki/FslInstallation</a>)            Jupyter Notebook 6.4.5 (Python 3.9.7 ipykernel) (<a href="https://jupyter.org">https://jupyter.org</a>)            R 4.2.0 (<a href="https://www.r-project.org">https://www.r-project.org</a>)            Python/3.10.8-GCCcore-12.2.0 (<a href="https://www.python.org">https://www.python.org</a>)            neuroCombat package in R (<a href="https://github.com/Jfortin1/ComBatHarmonization/tree/master/R">https://github.com/Jfortin1/ComBatHarmonization/tree/master/R</a>)</p> <p>Resting-state fMRI parcellations:            Schaefer et al. (2018) cortical parcellation (<a href="https://github.com/ThomasYeoLab/CBIG">https://github.com/ThomasYeoLab/CBIG</a>)            Fischl et al. (2002) subcortical segmentation (<a href="https://freesurfer.net/fswiki/SubcorticalSegmentation">https://freesurfer.net/fswiki/SubcorticalSegmentation</a>)</p>

For manuscripts utilizing custom algorithms or software that are central to the research but not yet described in published literature, software must be made available to editors and reviewers. We strongly encourage code deposition in a community repository (e.g. GitHub). See the Nature Portfolio [guidelines for submitting code & software](#) for further information.

## Data

Policy information about [availability of data](#)

All manuscripts must include a [data availability statement](#). This statement should provide the following information, where applicable:

- Accession codes, unique identifiers, or web links for publicly available datasets
- A description of any restrictions on data availability
- For clinical datasets or third party data, please ensure that the statement adheres to our [policy](#)

The ABCD data are publicly available via the NIMH Data Archive (NDA) and via <https://abcdstudy.org>. The HBN data are publicly available via Child Mind Institute Healthy Brain Network at [http://fcon\\_1000.projects.nitrc.org/indi/cmi\\_healthy\\_brain\\_network/Data.html](http://fcon_1000.projects.nitrc.org/indi/cmi_healthy_brain_network/Data.html). The HCP data are also publicly available and can be accessed via <https://www.humanconnectome.org>. Access to all three datasets require Data Use Agreement.

## Human research participants

Policy information about [studies involving human research participants and Sex and Gender in Research](#).

### Reporting on sex and gender

Across ABCD, HBN and HCP datasets, gender is self-reported. In our study, ABCD release 2.0.1 sample (N=5,260; female: 48.88%), HBN releases 1-7 (N=229; female: 42.36%) and HCP WU-Minn S1200 sample (N=423; female: 56.74%) Gender has been used as covariate as reported in the method section. Gender-based analysis has not been directly performed in this study.

### Population characteristics

ABCD release 2.0.1 sample (Age=119.27 months (SD=7.48), Race: 52.91% Caucasian, 13.63% African American, 20.72% Hispanic, 2.19% Asian, 10.42% Others) and HBN releases 1-7 (Age=14.73 years (SD=1.63), Race: 40.61% Caucasian, 16.59% African American, 11.35% Hispanic, 2.18% Asian, 0.44% Indian) HCP WU-Minn S1200 sample (Age=28.61 years (SD=3.72), Race: 77.66% Caucasian, 11.84% African American, 5.98% Asian/Hawaiian/Other Pacific Islanders, 0.27% Indian/Alaskan, 1.60% Other/Unreported)

### Recruitment

Information about ABCD recruitment is published: H. Garavan et al. Recruiting the ABCD sample: Design considerations and procedures. *Developmental Cognitive Neuroscience* (2018). <https://doi.org/10.1016/j.dcn.2018.04.004>. Information about HBN recruitment is published: Alexander LM et al. An open resource for transdiagnostic research in pediatric mental health and learning disorders. *Scientific Data* (2017). <https://doi.org/10.1038/sdata.2017.181> Information about HCP recruitment is published: Van Essen DC et al. The WU-Minn Human Connectome Project: an overview. *Neuroimage* (2013).

### Ethics oversight

Analyses were conducted according to the guidelines of the Yale University Human Subjects Committee

Note that full information on the approval of the study protocol must also be provided in the manuscript.

## Field-specific reporting

Please select the one below that is the best fit for your research. If you are not sure, read the appropriate sections before making your selection.

Life sciences  Behavioural & social sciences  Ecological, evolutionary & environmental sciences

For a reference copy of the document with all sections, see [nature.com/documents/nr-reporting-summary-flat.pdf](https://nature.com/documents/nr-reporting-summary-flat.pdf)

## Life sciences study design

All studies must disclose on these points even when the disclosure is negative.

### Sample size

Our analyses utilized publicly available ABCD, HBN and HCP neuroimaging and behavioral data. No sample size calculations were performed.

Sample size: ABCD data (N=5,260), HBN data (N=229) HCP data (N=423)

The final analytical sample of 5260 children from the ABCD study are those who were unrelated to each other, passed strict preprocessing quality control, had complete resting-state fMRI data and complete scores across all behavioral measures.

Following data processing and quality control, 412 participants aged between 12 and 18 years old from the HBN study releases 1-7 were available for analysis. Our final analytical sample consisted of 229 adolescents who did not differ from ABCD children in the levels of total internalizing and total externalizing problems.

After pre-processing quality control of imaging data, 752 participants from the HCP S1200 dataset had available scores across the complete set of structural and resting-state fMRI scans, as well as all behavioral scores of interest. Our main analysis comprised 423 adult participants, who did not differ from ABCD children in the levels of total internalizing and total externalizing problems

Since total internalizing and externalizing problems are the two main outcomes of interest whose associated predictive feature weights were

further examined in the current study, we focused our analyses on the subset of HBN and HCP participants who did not differ from the ABCD sample in the levels of total internalizing and externalizing problems. The complete set of HBN and HCP participants had significantly higher levels of total internalizing and externalizing problems than the ABCD sample because the HBN dataset was enriched for adolescents with psychiatric diagnoses, while ABCD children were aged 9-10 and very few received a psychiatric diagnosis at this age.

Data exclusions	We excluded subjects who failed preprocessing quality control, had incomplete resting-state fMRI data and incomplete behavioral scores.
Replication	Our study did not conduct any replication analyses because our study involved three different samples from three different datasets which have different geographical and family structures to each other. For this reason, it is impossible to apply the KRR model trained in one sample to the other ones directly. However, we used KRR models to predict behavioral measures which assess the same set of internalizing and externalizing behaviors across the three datasets after adapting the implementation of KRR models according to the structure of each dataset.
Randomization	We utilized the publicly available ABCD, HBN and HCP datasets in our study, which was not randomized. Randomization is not pertinent to our current investigation, as the statistical method employed (kernel ridge regression and exact test of differences) does not necessitate randomization.
Blinding	Blinding is not relevant to this study as no data collection was involved and participants were not assigned to different groups. Our research question and analysis pipeline did not involve group comparisons and all behavioral measures of interest were assessed as self-reported dimensions.

## Reporting for specific materials, systems and methods

We require information from authors about some types of materials, experimental systems and methods used in many studies. Here, indicate whether each material, system or method listed is relevant to your study. If you are not sure if a list item applies to your research, read the appropriate section before selecting a response.

### Materials & experimental systems

### Methods

n/a	Involved in the study
<input checked="" type="checkbox"/>	<input type="checkbox"/> Antibodies
<input checked="" type="checkbox"/>	<input type="checkbox"/> Eukaryotic cell lines
<input checked="" type="checkbox"/>	<input type="checkbox"/> Palaeontology and archaeology
<input checked="" type="checkbox"/>	<input type="checkbox"/> Animals and other organisms
<input checked="" type="checkbox"/>	<input type="checkbox"/> Clinical data
<input checked="" type="checkbox"/>	<input type="checkbox"/> Dual use research of concern

n/a	Involved in the study
<input checked="" type="checkbox"/>	<input type="checkbox"/> ChIP-seq
<input checked="" type="checkbox"/>	<input type="checkbox"/> Flow cytometry
<input type="checkbox"/>	<input checked="" type="checkbox"/> MRI-based neuroimaging

## Magnetic resonance imaging

### Experimental design

Design type	resting-state functional magnetic resonance imaging
Design specifications	ABCD: 20 minutes of resting-state fMRI data, consisting of four 5-minute runs, was collected from each ABCD child participant (TR=800ms) HBN: one 10.3 minutes of resting-state fMRI run (TR=1450ms; Staten Island site) or two 5.1 minutes of resting-state fMRI runs (TR=800ms; Rutgers and CBIC sites) HCP: four 15-minute resting-state fMRI sessions (TR=2400ms) with opposite phase encoding directions (two sessions of L/R and two sessions of R/L)
Behavioral performance measures	Our study utilized resting-state fMRI data which does not involve any behavioral performance measures.

### Acquisition

Imaging type(s)	resting-state functional MRI
Field strength	3T
Sequence & imaging parameters	ABCD: Resolution: 2.4x2.4x2.4 mm; FOV: 216x216; Matrix Size: 90x90; Duration: 20 minutes (1500 timepoints); TR: 800ms; TE: 30ms; Multiband EPI acceleration: 6; flip angle: 52°. Further details have been published: Casey BJ et al; ABCD Imaging Acquisition Workgroup. The Adolescent Brain Cognitive Development (ABCD) study: Imaging acquisition across 21 sites. Dev Cogn Neurosci (2018). HBN: Resolution: 2.5x2.5x2.5 mm (Staten Island site) or 2.4x2.4x2.4 mm (CBIC and Rutgers); FOV:216x216; acquisition matrix = 90 x 90; TR/TE: 800/30 (CBIC and Rutgers) or 1450/40 (Staten Island); Duration: one 10-minute scan (Staten Island) or two 5-minute scans (CBIC and Rutgers). Further details have been published: Alexander LM et al. An open resource for transdiagnostic research in pediatric mental health and learning disorders. Scientific Data (2017). <a href="https://doi.org/10.1038/sdata.2017.181">https://doi.org/10.1038/sdata.2017.181</a> HCP: Resolution: 2x2x2mm; FOV: 208mm in the read direction (anterior-posterior), 180mm in the phase encoding direction (L-R or R-L; a 104x90 matrix) and 144mm in the inferior-superior direction; Duration: 60 minutes (1500 time

points); phase encoding directions: L/R (two 15-minute sessions) and R/L (two 15-minute sessions); TR:720ms; TE:33ms; Multiband EPI acceleration: 8; flip angle: 52°. Further details have been published: Smith SM et al; WU-Minn HCP Consortium. Resting-state fMRI in the Human Connectome Project. *Neuroimage* (2013), and Uğurbil K et al; WU-Minn HCP Consortium. Pushing spatial and temporal resolution for functional and diffusion MRI in the Human Connectome Project. *Neuroimage* (2013).

Area of acquisition

Whole brain

Diffusion MRI

 Used Not used

## Preprocessing

Preprocessing software

ABCD and HBN: FreeSurfer 5.3.0 and FMRIB Software Library (FSL) 5.8.0.  
HCP: HCP minimal preprocessing pipelines (S1200 release, march 2017). Further details have been published at Glasser MF et al; WU-Minn HCP Consortium. The minimal preprocessing pipelines for the Human Connectome Project. *Neuroimage* (2013).

Normalization

ABCD and HBN: projected onto FreeSurfer fsaverage6 surface space  
HCP: Native fMRI volumes went through nonlinear registration to the MNI space and mapped to the standard CIFTI grayordinate coordinate space

Normalization template

ABCD: FreeSurfer fsaverage6 surface space  
HBN: FreeSurfer fsaverage6 surface space  
HCP: 2mm MNI space

Noise and artifact removal

ABCD: used linear regression to remove quadratic trends, signals correlated with estimated motion time courses, and the mean time courses of cerebral white matter, ventricles, and whole brain, as well as their first derivatives. Motion regression includes six parameters plus their derivatives and squares. Further details have been published at Hagler DJ Jr et al. Image processing and analysis methods for the Adolescent Brain Cognitive Development Study. *Neuroimage* (2019).  
HBN: frames with FD > 0.3mm or DVARS > 60 were flagged as censored frames. 1 frame before and 2 frames after these volumes were flagged as censored frames. Uncensored segments of data lasting fewer than five contiguous frames were also labeled as censored frames. BOLD runs with over half of the frames censored and runs with max FD > 5mm were removed. The data was then corrected for susceptibility-induced spatial distortion and regressed out a vector of ones and linear trend, global signal, six motion correction parameters, averaged ventricular signal, averaged white matter signal, and their temporal derivatives.  
HCP: Each fMRI timepoint has a unique transformation driven by its 6 DOF motion correction matrix. Before regressing out the 6 motion parameters, gradient nonlinearity distortion correction is applied. After that, EPI distortion correction is applied. Further details have been published at Glasser MF et al; WU-Minn HCP Consortium. The minimal preprocessing pipelines for the Human Connectome Project. *Neuroimage* (2013).

Volume censoring

ABCD: Removal of initial frames depends on the type of scanner. On Siemens and Philips scanners, the first eight frames make up the pre-scan reference, and are not saved as DICOMS. An additional eight frames are discarded as part of the pre-analysis processing, for a total of 16 initial frames. On GE scanners with software version DV25, the first 12 frames make up the pre-scan reference. Instead of being discarded, those 12 reference scans are combined into one, and saved as the first frame, for a total of five initial frames to be discarded as part of the pre-analysis processing for GE DV25 series. On GE scanners with software version DV26, the pre-scan reference is not retained at all, and a total of 16 initial frames are discarded for GE DV26 scans as part of the pre-analysis processing. Volumes with FD > 0.3 mm or DVARS > 50, along with one volume before and two volumes after, were flagged as outliers. Uncensored segments of data having fewer than 5 contiguous volumes were also flagged as outliers and censored. Further details have been published at Hagler DJ Jr et al. Image processing and analysis methods for the Adolescent Brain Cognitive Development Study. *Neuroimage* (2019).  
HBN: removal of the first eight frames. Frames with FD > 0.3mm or DVARS > 60 were flagged as censored frames. One frame before and two frames after these volumes were flagged as censored frames. Uncensored segments of data lasting fewer than five contiguous frames were also labeled as censored frames  
HCP: no volume censoring. Further details have been published at Glasser MF et al; WU-Minn HCP Consortium. The minimal preprocessing pipelines for the Human Connectome Project. *Neuroimage* (2013).

## Statistical modeling & inference

Model type and settings

Our study utilized resting-state fMRI data which does not assess task-related contrasts.

Effect(s) tested

Our study utilized resting-state fMRI data which does not assess any task-related effects.

Specify type of analysis:

Whole brain

ROI-based

Both

Anatomical location(s)

ROIs were defined using the Schaefer cortical and Freesurfer subcortical.  
Schaefer, A. et al. Local-global parcellation of the human cerebral cortex from intrinsic functional connectivity MRI. *Cereb. Cortex* 28, 3095–3114 (2018).  
Fischl, B. et al. Whole brain segmentation: automated labeling of neuroanatomical structures in the human brain. *Neuron* 33, 341–355 (2002).

Statistic type for inference  
(See [Eklund et al. 2016](#))

Analyses were conducted at the level of resting-state functional connectivity between individual parcels.

Correction

Where relevant, statistical tests were corrected for multiple comparisons.

## Models & analysis

n/a | Involved in the study

- Functional and/or effective connectivity
- Graph analysis
- Multivariate modeling or predictive analysis

Functional and/or effective connectivity

Functional connectivity was measured by Pearson's  $r$  correlations between the mean time series of each pair of ROIs.

Multivariate modeling and predictive analysis

ABCD: we used kernel ridge regression models to predict each behavioral measure from subject-specific resting-state functional connectivity matrices. To evaluate predictive accuracy, we performed leave-3-site-clusters-out nested cross-validation for each behavioral measure. At each fold, a different set of 3 site-categories served as the test set, and the remaining 5 site-categories were used as the training set, resulting in 56 folds in total. Pearson's correlation between predicted and actual behavioral scores was used as accuracy metrics. Statistical significance of prediction accuracy was assessed by permutation testing.  
HBN: We used kernel ridge regression models to predict each behavioral measure from subject-specific resting-state functional connectivity matrices. To evaluate predictive accuracy, we implemented 60 random initiations of 10-fold nested cross-validation. Pearson's correlation between predicted and actual behavioral scores and coefficient of determination were used as accuracy metrics. Statistical significance of prediction accuracy was assessed by permutation testing.  
HCP: We used kernel ridge regression models to predict each behavioral measure from subject-specific resting-state functional connectivity matrices. To evaluate predictive accuracy, we implemented 60 random initiations of 10-fold nested cross-validation. Pearson's correlation between predicted and actual behavioral scores and coefficient of determination were used as accuracy metrics. Statistical significance of prediction accuracy was assessed by permutation testing.